

## A SIMPLE PREDICTION FORMULA OF ROLL DAMPING OF CONVENTIONAL CARGO SHIPS ON THE BASIS OF IKEDA'S METHOD AND ITS LIMITATION

Yuki KAWAHARA, Kazuya MAEKAWA, Yoshiho IKEDA  
Department of Marine System Engineering,  
Osaka Prefecture University Sakai, Japan  
ikedata@marine.osakafu-u.ac.jp

### ABSTRACT

Since the roll damping of ships has significant effects of viscosity, it is difficult to calculate it theoretically. Therefore experimental results or some prediction methods are used to get the roll damping in design stage of ships. Among some prediction methods, Ikeda's one is widely used in many ship motion computer programs.

Using the method, the roll damping of various ship hulls with various bilge keels are calculated to investigate its characteristics. Ship hull forms are systematically changed by changing length, beam, draft, midship sectional coefficient and prismatic coefficient.

On the basis of these predicted roll damping of various ships, a very simple prediction formula of the roll damping of ships is deduced. It is found, however, that this formula cannot be used for ships that have high position of the center of gravity. A modified method to improve accuracy for such ships is proposed.

**Keywords:** *Roll Damping, Simple Prediction Formula, Wave component, Eddy component, Bilge keel component*

### 1. INTRODUCTION

In 1970's, strip methods for predicting ship motions in 5-degree of freedoms in waves have been established. The methods are based on potential flow theories (Ursell-Tasai method, source distribution method and etc), and can predict pitch, heave, sway and yaw motions of ships in waves in fairly good accuracy. In roll motion, however, the strip methods do not work well because of significant viscous effects on the roll damping. Therefore, some empirical formulas or experimental data are used to predict the roll damping in the strip methods.

To improve the prediction of roll motions by these strip methods, one of the authors carried out a research project to develop a roll

damping prediction method which has the same concept and the same order of accuracy as the strip methods which are based on hydrodynamic forces acting on strips, or cross sections of a ship [Ikeda et al. (1976), Ikeda et al. (1977a), Ikeda et al. (1977b), Ikeda et al. (1978): All papers in English versions were published as Reports of Dept. of Naval Architecture, Univ. of Osaka Pref.]. The review of the prediction method was made by Himeno (1981) and Ikeda (1982) with the computer program.

The prediction method, which is now called Ikeda's method, divides the roll damping into the frictional (BF), the wave ( $B_W$ ), the eddy ( $B_E$ ) and the bilge keel ( $B_{BK}$ ) components at zero forward speed, and at forward speed, the lift ( $B_L$ ) is added. Increases of wave and

friction components due to advance speed are also corrected on the basis of experimental results. Then the roll damping coefficient  $B_{44}$  (=Roll damping moment (kgfm) / Roll angular velocity (rad/sec) ) can be expressed as follows.

$$B_{44} = B_F + B_W + B_E + B_L + B_{BK} \quad (1)$$

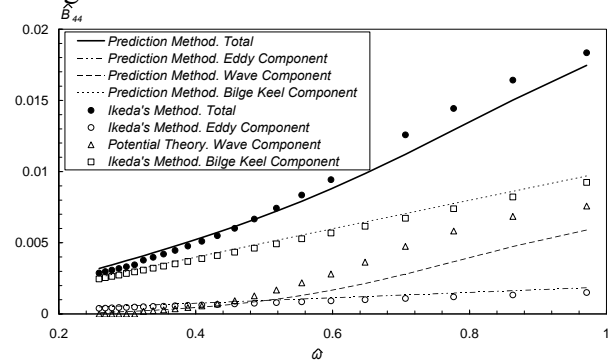
At zero forward speed, each component except the friction component is predicted for each cross section with unit length and the predicted values are summed up along the ship length. The friction component is predicted by Kato's formula for a three-dimensional ship shape. Modification functions for predicting the forward speed effects on the roll damping components are developed for the friction, wave and eddy components. The computer program of the method was published, and the method has been widely used.

For these thirty years, the original Ikeda's method developed for conventional cargo ships has been improved to apply many kinds of ships, for examples, more slender and round ships, fishing boats, barges, ships with skegs and so on. The original method is also widely used. However, sometimes, different conclusions of roll motions were derived even though the same Ikeda's method was used in the calculations. Then, to check the accuracy of the computer programs of the same Ikeda's method, a more simple prediction method with the almost same accuracy as the Ikeda's original one has been expected to be developed. It is said that in design stages of ships, Ikeda's method is too complicated to use. To meet these needs, a simple roll damping prediction method was deduced by using regression analysis [Kawahara et al. (2008)].

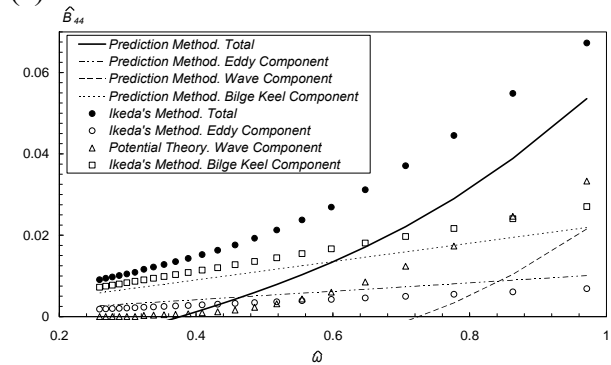
## 2. PREVIOUS PREDICTION FORMULA

The simple prediction formula proposed in previous paper cannot be used for modern ships that have high position of center of gravity or long natural roll period such as large passenger ships with relatively flat hull shape.

In order to investigate its limitation, the authors compared with the result of this prediction method and original Ikeda's one out of its calculating limitation. Figure 1 shows the result of the comparison with their method of roll damping. The upper one is on the condition that the center of gravity is low and the lower one on the condition that the center of gravity is high.



(a)  $OG/d = -0.2$



(b)  $OG/d = -1.5$

Figure 1. Comparison between Ikeda's method and proposed one of roll damping at  $L/B=6.0$ ,  $B/d=4.0$ ,  $C_b=0.65$ ,  $C_m=0.98$ ,  $\phi_a=10^\circ$ ,  $b_{BK}/B=0.025$  and  $l_{BK}/L_{pp}=0.2$ . ( $OG$  denotes the distance between water surface and center of gravity, and defined plus when the center of gravity is below water surface.)

From this figure, the roll damping estimated by this prediction formula are in good agreement with the roll damping calculated by the Ikeda's method for low position of center of gravity, but the error margin grows for the high position of center of gravity. The results suggest that the previous prediction formula is necessary to be revised.

### 3. METHODOICAL SERIES SHIPS

Modified prediction formula will be developed on the basis of the predicted results by Ikeda's method using the methodical series ships. This series ships are constructed based on the Taylor Standard Series and its hull shapes are methodically changed by changing length, beam, draft, midship sectional coefficient and longitudinal prismatic coefficient. The geometries of the series ships are given by the following equations.

$$y_1 = Q(x) + C_P P(x) + f_{11} t T(x) + n N(x) + f_{12} F(x) \quad (2)$$

$$y_2 = Q(x) + C_W P(x) + f_{21} t T(x) + n N(x) + f_{22} F(x) \quad (3)$$

where

$$Q(x) = -30x^2 + 100x^3 - 105x^4 + 36x^5 \quad (4)$$

$$P(x) = 60x^2 - 180x^3 + 180x^4 - 60x^5 \quad (5)$$

$$T(x) = x - 6x^2 + 12x^3 - 10x^4 + 3x^5 \quad (6)$$

$$N(x) = -0.5x^2 + 2x^3 - 2.5x^4 + x^5 \quad (7)$$

$$F(x) = -26.562x^6 + 105.74x^5 - 162.71x^4 + 116.58x^3 - 34.532x^2 + 0.6998x + 0.7923 \quad (8)$$

$$t = -3969.7C_P^6 + 16664.6C_P^5 - 28230C_P^4 + 24951C_P^3 - 12205C_P^2 + 3147.7C_P - 335.67 \quad (9)$$

(at stern side and  $C_P < 0.73$ )

$$t = 113.64C_P^2 - 149.68C_P + 50.221 \quad (10)$$

(at stern side and  $C_P \geq 0.73$ )

$$t = 96.339C_P^5 - 173.59C_P^4 + 159.75C_P^3 - 113.4C_P^2 + 54.123C_P - 10.686 \quad (11)$$

(at bow side and  $C_P < 0.72$ )

$$t = 41.667C_P^2 - 49.167C_P + 14.9 \quad (12)$$

(at bow side and  $C_P \geq 0.72$ )

$$n = 5.7035C_P^3 - 30.16C_P^2 + 33.471C_P - 10.606 \quad (13)$$

(at stern side and  $C_P < 0.74$ )

$$n = -10.417C_P^2 + 13.458C_P - 4.305 \quad (14)$$

(at stern side and  $C_P \geq 0.74$ )

$$n = -1664.6C_P^5 + 5596.7C_P^4 - 7413.2C_P^3 + 4815.6C_P^2 - 1525.3C_P + 186.79 \quad (15)$$

(at bow side and  $C_P < 0.73$ )

$$n = 0.625C_P + 0.4312 \quad (16)$$

(at bow side and  $C_P \geq 0.73$ )

where

$y_1$  is the non-dimensional value obtained by sectional-immersed-area divided by maximum-immersed-area,

$y_2$  is the non-dimensional value obtained by sectional-water-line-breadth divided by maximum-water-line-breadth,

$x$  is the non-dimensional value of longitudinal position when  $x$  is measured from the extremity of either the bow or stern,

$C_P$  is the longitudinal prismatic coefficient,

$C_W$  is the water-plane coefficient,

$f_{11}$  is constant and equal to 0.6 for the stern and 1.0 for the bow,

$f_{12}$  is constant and equal to 0.05,

$f_{21}$  is constant and equal to 2.0 for the stern and 1.0 for the bow,

$f_{22}$  is constant and equal to 0.15 for the stern and 0.1 for the bow.

However, occasionally, corrections of the results obtained from the Eqs.2, 3 are required. For example, if maximum of  $y_1$  exceeds 1.0, it is adjusted to 1.0.

Figures 2 and 3 show the sectional area curves obtained from Eq.2 and a body plan of a ship with  $C_b=0.84$  ( $C_b$  : block coefficient) and  $C_m=0.98$  ( $C_m$  : midship section coefficient), respectively. Since the hull shapes used here are conventional ones as shown in Figure 3, an application of the deduced prediction method to modern unconventional hull shapes, for example buttock-flow hull, should be careful.

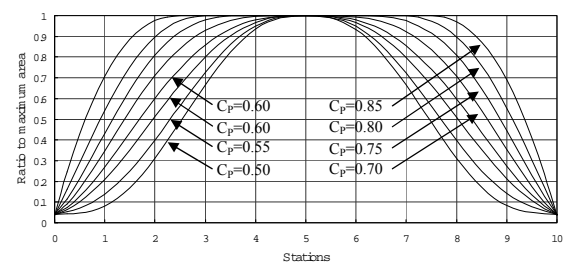


Figure 2. Sectional-area curves of series model used in calculation.

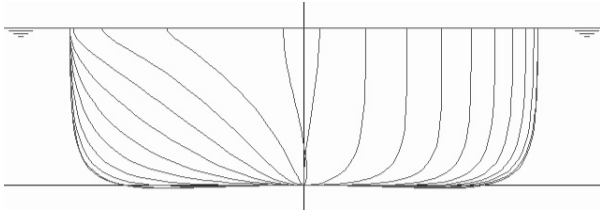


Figure 3. An example of body plan of ship with  $C_b=0.84$  and  $C_m=0.98$ .

#### 4. PROPOSAL OF NEW PREDICTION METHOD OF ROLL DAMPING

In this chapter, the characteristics of each component of the roll damping, the frictional, the wave, the eddy and the bilge keel components at zero advanced speed, are discussed, and a simple prediction formula of each component is developed.

The roll damping coefficient ( $B_{44}$ ) and circular frequency ( $\omega=2\pi/T_w$ ) are defined as follows,

$$\mathcal{B}_{44} = \frac{B_{44}}{\rho \nabla B^2} \sqrt{\frac{B}{2g}} \quad (17)$$

$$\mathcal{G} = \omega \sqrt{\frac{B}{2g}} \quad (18)$$

where  $\rho$  denotes water density,  $\nabla$  displacement volume,  $B$  beam and  $g$  is gravity acceleration, respectively.

The relationship between  $B_{44}$  and  $N$  coefficient (Bertin) is as follows.

$$N = \mathcal{B}_{44} \frac{\pi B \mathcal{G}}{GM \varphi_a} \quad (\varphi_a \text{ in Eq.19 is in deg.}) \quad (19)$$

##### 4.1 Frictional Component ( $B_F$ )

In Ikeda's method, the friction damping at  $F_n=0$  is given by Kato's formula as follows,

$$B_F = \frac{4}{3\pi} \rho s_f r_f^3 \varphi_a \omega c_f \quad (20)$$

where  $c_f$  is frictional coefficient,  $r_f$  is average radius from the axis of rolling and  $s_f$  is wetted

surface area. These parameters in the equation are given by the following equations,

$$c_f = 1.328 \left( \frac{3.22 r_f^2 \varphi_a^2}{T \nu} \right)^{\frac{1}{2}} \quad (21)$$

$$r_f = \frac{(0.887 + 0.145 C_b)(1.7d + C_b B) - 2OG}{\pi} \quad (22)$$

$$s_f = L_{PP}(1.75d + C_b B) \quad (23)$$

where  $\varphi_a$  denotes roll amplitude,  $T$  roll period,  $\nu$  dynamic coefficient of viscosity,  $OG$  distance from calm water surface to the axis of rolling (downward direction is positive) and  $d$  draft, respectively.

In the present study, since the frictional component of roll damping is already given for a whole ship as Eqs.20-23, the formula is used without any modification in the simple prediction method developed in the present study. It should be noted, however, the frictional component is negligible for a full-scale ship although it takes about 5-10% of the total roll damping for a small scale model.

##### 4.2 Wave Component ( $B_W$ )

As well known, the wave component of the roll damping for a two-dimensional cross section can be calculated by potential flow theories in fairly good accuracy. In Ikeda's method, the wave damping of a strip section is not calculated and the calculated values by any potential flow theories are used as the wave damping.

##### 4.2.1 Characteristics of the Wave Component

The reason why viscous effects are significant in only roll damping can be explained as follows. Figure 4 shows the wave component of the roll damping for 2-D sections calculated by a potential flow theory. We can see that the component is very small for sections with half breadth / draft ratio,  $H_0=0.5-1.5$ , particularly when area coefficient,  $\sigma$  is large. Usually, conventional ships have such  $H_0$

at parallel middle body part. Then ships have relatively small wave roll damping, and viscous effects play an important role in the roll damping.

In Figures 5 and 6, calculated distributions of the wave component of the roll damping are shown. The results for a full ship ( $C_b=0.8$ ) shown in Figure 5 demonstrate that the damping created by the mid-ship body is very small, and that created by the stern body is large. The results for a slender ship ( $C_b=0.5$ ) shows two peaks at the cross sections of  $SS=3$  and  $SS=7$ . The reason why the peaks appear on bow and stern parts can be easily understood from the calculated results shown in Figure 4.

Dependencies of the wave component on location of roll axis or center of gravity are shown in Figure 7.

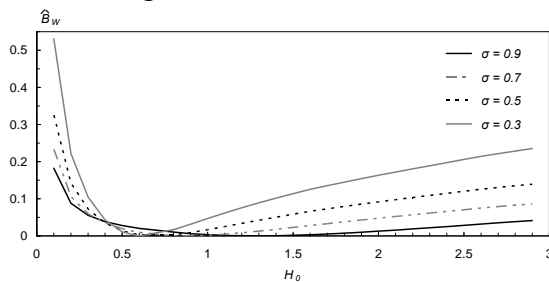


Figure 4. Characteristics of roll damping coefficient of wave component for two-dimensional section at  $OG/d=0$  and  $\bar{\phi}=1.25$ .

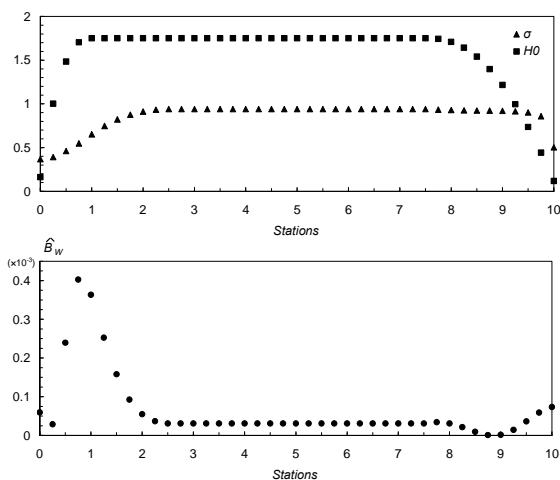


Figure 5 Longitudinal distribution of  $\sigma$ ,  $H_0$  and roll damping coefficient of wave component for a ship with  $L/B=5$ ,  $B/d=3.5$ ,  $C_m=0.94$ ,  $C_b=0.8$ ,  $OG/d=0$  and  $\bar{\phi}=1.25$ .

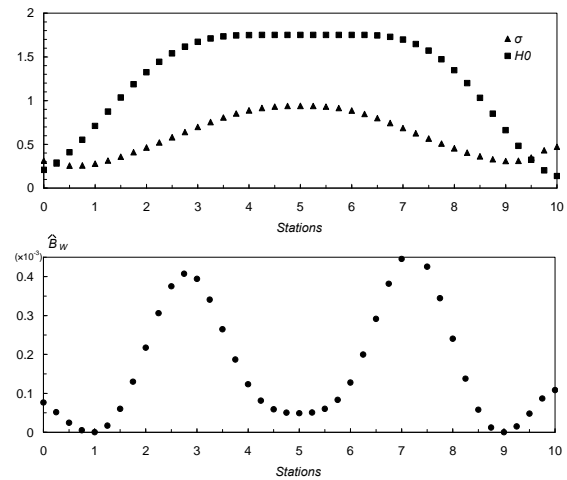


Figure 6. Longitudinal distribution of  $\sigma$ ,  $H_0$  and roll damping coefficient of wave component for a ship with  $L/B=5$ ,  $B/d=3.5$ ,  $C_m=0.94$ ,  $C_b=0.5$ ,  $OG/d=0$  and  $\bar{\phi}=1.25$ .

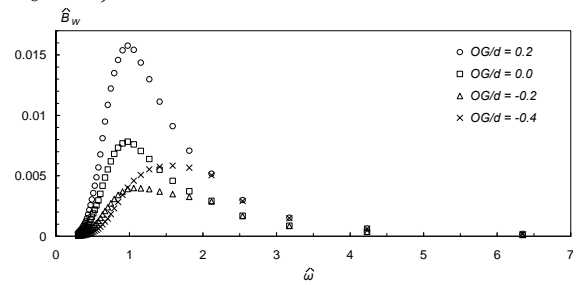


Figure 7. Characteristics of roll damping coefficient of wave component for a whole ship at  $L/B=5$ ,  $B/d=3.5$ ,  $C_m=0.94$ ,  $C_b=0.8$ .

#### 4.2.2 Proposed Formula of the Wave Roll Damping

By fitting these predicted wave components a simple prediction formula is deduced as follows.

$$\begin{aligned}
 x_1 &= B/d, \quad x_2 = C_b, \quad x_3 = C_m, \quad x_4 = 1 - OG/d, \quad x_5 = \bar{\mu} \\
 \bar{B}_w &= A_1/x_5 \cdot \exp(-A_2(\log(x_5) - A_3)^2/1.44) \\
 A_1 &= (A_{11}x_4^2 + A_{12}x_4 + A_{13})AA_1 \\
 A_2 &= -1.402x_4^3 + 7.189x_4^2 - 10.993x_4 + 9.45 \\
 A_3 &= A_{31}x_4^6 + A_{32}x_4^5 + A_{33}x_4^4 + A_{34}x_4^3 + A_{35}x_4^2 + A_{36}x_4 + A_{37} + AA_3 \\
 x_6 &= x_4 - AA_{32} \\
 AA_1 &= (AA_{11}x_3 + AA_{12}) \times (1 - x_4) + 1.0 \\
 AA_3 &= AA_{31}(-1.05584x_6^9 + 12.688x_6^8 - 63.70534x_6^7 + \\
 &\quad 172.84571x_6^6 - 274.05701x_6^5 + 257.68705x_6^4 - 141.40915x_6^3 \\
 &\quad + 44.13177x_6^2 - 7.1654x_6 - 0.0495x_1^2 + 0.4518x_1 - 0.61655) \\
 AA_{31} &= (-0.3767x_1^3 + 3.39x_1^2 - 10.356x_1 + 11.588) \cdot AA_{311} \\
 AA_{32} &= -0.0727x_1^2 + 0.7x_1 - 1.2818 \\
 AA_{311} &= (-17.102x_2^3 + 41.495x_2^2 - 33.234x_2 + 8.8007) \cdot x_4 + \\
 &\quad 36.566x_2^3 - 89.203x_2^2 + 71.8x_2 - 18.108 \\
 A_{31} &= -7686.0287x_2^6 + 30131.5678x_2^5 - 49048.9664x_2^4 + \\
 &\quad 42480.7709x_2^3 - 20665.147x_2^2 + 5355.2035x_2 - 577.8827 \\
 A_{32} &= 61639.9103x_2^6 - 241201.0598x_2^5 + 392579.5937x_2^4 - \\
 &\quad 340629.4699x_2^3 + 166348.6917x_2^2 - 43358.7938x_2 + 4714.7918 \\
 A_{33} &= -130677.4903x_2^6 + 507996.2604x_2^5 - 826728.7127x_2^4 \\
 &\quad + 722677.104x_2^3 - 358360.7392x_2^2 \\
 &\quad + 95501.4948x_2 - 10682.8619 \\
 A_{34} &= -110034.6584x_2^6 + 446051.22x_2^5 - 724186.4643x_2^4 \\
 &\quad + 599411.9264x_2^3 - 264294.7189x_2^2 \\
 &\quad + 58039.7328x_2 - 4774.6414 \\
 A_{35} &= 709672.0656x_2^6 - 2803850.2395x_2^5 + 4553780.5017x_2^4 \\
 &\quad - 3888378.9905x_2^3 + 1839829.259x_2^2 \\
 &\quad - 457313.6939x_2 + 46600.823 \\
 A_{36} &= -822735.9289x_2^6 + 3238899.7308x_2^5 - 5256636.5472x_2^4 \\
 &\quad + 4500543.147x_2^3 - 2143487.3508x_2^2 \\
 &\quad + 538548.1194x_2 - 55751.1528
 \end{aligned}$$

$$\begin{aligned}
 A_{37} &= 299122.8727x_2^6 - 1175773.1606x_2^5 + 1907356.1357x_2^4 \\
 &\quad - 1634256.8172x_2^3 + 780020.9393x_2^2 \\
 &\quad - 196679.7143x_2 + 20467.0904 \\
 AA_{11} &= AA_{111}x_2^2 + AA_{112}x_2 + AA_{113} \\
 AA_{12} &= AA_{121}x_2^2 + AA_{122}x_2 + AA_{123} \\
 AA_{111} &= 17.945x_1^3 - 166.294x_1^2 + 489.799x_1 - 493.142 \\
 AA_{112} &= -25.507x_1^3 + 236.275x_1^2 - 698.683x_1 + 701.494 \\
 AA_{113} &= 9.077x_1^3 - 84.332x_1^2 + 249.983x_1 - 250.787 \\
 AA_{121} &= -16.872x_1^3 + 156.399x_1^2 - 460.689x_1 + 463.848 \\
 AA_{122} &= 24.015x_1^3 - 222.507x_1^2 + 658.027x_1 - 660.665 \\
 AA_{123} &= -8.56x_1^3 + 79.549x_1^2 - 235.827x_1 + 236.579 \\
 A_{11} &= A_{111}x_2^2 + A_{112}x_2 + A_{113} \\
 A_{12} &= A_{121}x_2^3 + A_{122}x_2^2 + A_{123}x_2 + A_{124} \\
 A_{13} &= A_{131}x_2^3 + A_{132}x_2^2 + A_{133}x_2 + A_{134} \\
 A_{111} &= -0.002222x_1^3 + 0.040871x_1^2 - 0.286866x_1 + 0.599424 \\
 A_{112} &= 0.010185x_1^3 - 0.161176x_1^2 + 0.904989x_1 - 1.641389 \\
 A_{113} &= -0.015422x_1^3 + 0.220371x_1^2 - 1.084987x_1 + 1.834167 \\
 A_{121} &= -0.0628667x_1^4 + 0.4989259x_1^3 + 0.52735x_1^2 \\
 &\quad - 10.7918672x_1 + 16.616327 \\
 A_{122} &= 0.1140667x_1^4 - 0.8108963x_1^3 - 2.2186833x_1^2 \\
 &\quad + 25.1269741x_1 - 37.7729778 \\
 A_{123} &= -0.0589333x_1^4 + 0.2639704x_1^3 + 3.1949667x_1^2 \\
 &\quad - 21.8126569x_1 + 31.4113508 \\
 A_{124} &= 0.0107667x_1^4 + 0.0018704x_1^3 - 1.2494083x_1^2 \\
 &\quad + 6.9427931x_1 - 10.2018992 \\
 A_{131} &= 0.192207x_1^3 - 2.787462x_1^2 + 12.507855x_1 - 14.764856 \\
 A_{132} &= -0.350563x_1^3 + 5.222348x_1^2 - 23.974852x_1 + 29.007851 \\
 A_{133} &= 0.237096x_1^3 - 3.535062x_1^2 + 16.368376x_1 - 20.539908 \\
 A_{134} &= -0.067119x_1^3 + 0.966362x_1^2 - 4.407535x_1 + 5.894703 \\
 &\quad \left( \begin{aligned} &0.5 \leq C_b \leq 0.85, \quad 2.5 \leq B/d \leq 4.5, \quad \bar{\mu} \leq 1.0 \\ &-1.5 \leq OG/d \leq 0.2, \quad 0.9 \leq C_m \leq 0.99 \end{aligned} \right)
 \end{aligned}$$

(24)

### 4.3 Eddy Component ( $B_E$ )

The eddy component of the roll damping is created by small separation bubbles or small shedding vortices generated at the bilge part of midship section and large vortices generated at the relatively sharp bottom of bow and stern sections. Although vortex shedding flow from oscillating bluff bodies is usually govern by Keulegan-Carpenter number,  $Kc$ , it was found by Ikeda et al.(1978b) that the viscous forces created by such small separation bubbles or small shedding vortices do not significantly



depend on  $K_c$ . In Ikeda's prediction method, the distribution of the pressure created on a hull surface by such separation bubble is assumed as a simple shape for each shape of cross sections on the basis of experimental results of pressure distribution on hull surfaces. The pressure value was determined as the calculated eddy components of the roll damping for various cross sections are in good agreement with measured ones. Then, the eddy damping of a strip section is calculated by following formulas.

$$B'_E = \frac{4}{3\pi} \rho L_{PP} d^2 r_{\max}^2 \varphi_a \omega \left\{ \left( 1 - f_1 \frac{R}{d} \right) \left( 1 - \frac{OG}{d} - f_1 \frac{R}{d} \right) + f_2 \left( H_0 - f_1 \frac{R}{d} \right)^2 \right\} C_{P0} \quad (25)$$

$$f_1 = \frac{1}{2} [1 + \tanh \{20(\sigma - 0.7)\}] \quad (26)$$

$$f_2 = \frac{1}{2} (1 - \cos \pi \sigma) - 1.5 (1 - e^{-5(1-\sigma)}) \sin^2 \pi \sigma \quad (27)$$

$$C_{P0} = \frac{1}{2} (0.87 e^{-\gamma} - 4 e^{-0.1877} + 3) \quad (28)$$

$$H_0 = \frac{B}{2d} \quad (29)$$

$$\sigma = \frac{S}{Bd} \quad (30)$$

where,  $r_{\max}$  is maximum distance from center of gravity (roll axis) to hull surface,  $R$  is bilge radius and  $\sigma$  is sectional area coefficient.

The eddy roll damping of a whole ship is calculated by integrating  $B'_E$  to longitudinal direction.

#### 4.3.1 Characteristics of Eddy Component

In Figures 8 and 9, the longitudinal distribution of the predicted eddy component of the roll damping are shown for a slender ship ( $C_b=0.5$ ) and a full ship ( $C_b=0.8$ ). The eddy component of a slender ship is large at bow and stern parts, and has a small peak at mid-ship, as shown in Figure 8. For a full ship, however, the eddy damping at parallel middle body part becomes larger and longer as shown in Figure 9. The component at stern is large as

a slender ship, but becomes small at bow part. These may be caused by that both ships has similar V shape stern but the full ship has U shape bow section which is not thin and flat shape as a slender ship.

Figure 10 shows the effect of midship-section coefficient ( $C_m$ ) on the eddy damping. The results demonstrate that the eddy component of the roll damping of parallel body parts of ships is significantly sensitive to  $C_m$ . This is because of larger flow separation occurs at bilge corners of ships with large midship-section coefficient.

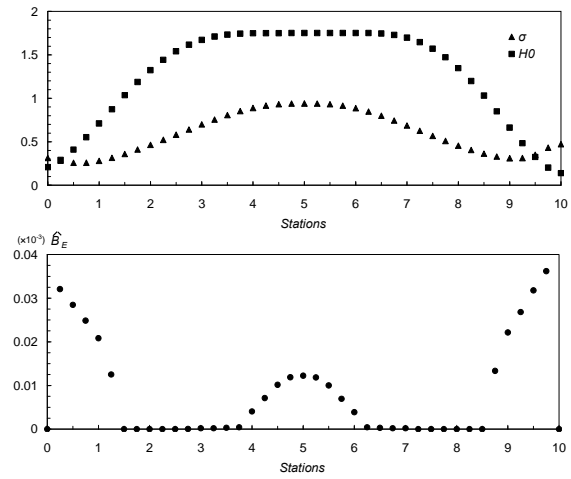


Figure 8. Longitudinal distribution of  $\sigma$ ,  $H_0$  and roll damping coefficient of eddy component for a ship with  $L/B=5$ ,  $B/d=3.5$ ,  $C_m=0.94$ ,  $C_b=0.5$ ,  $OG/d=0$  and  $\phi=1.25$ .

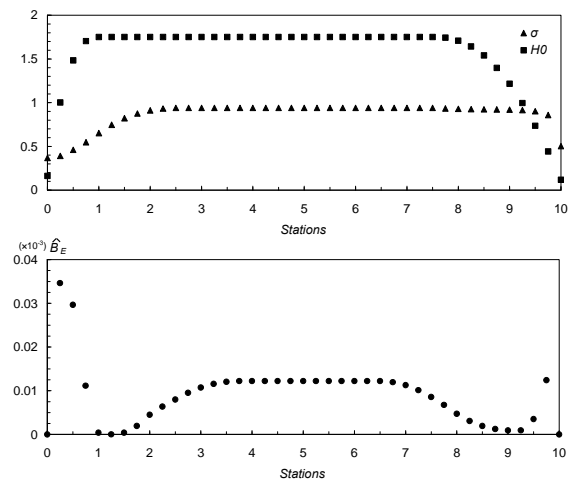


Figure 9. Longitudinal distribution of  $\sigma$ ,  $H_0$  and roll damping coefficient of eddy component for a ship with  $L/B=5$ ,  $B/d=3.5$ ,  $C_m=0.94$ ,  $C_b=0.8$ ,  $OG/d=0$  and  $\phi=1.25$ .

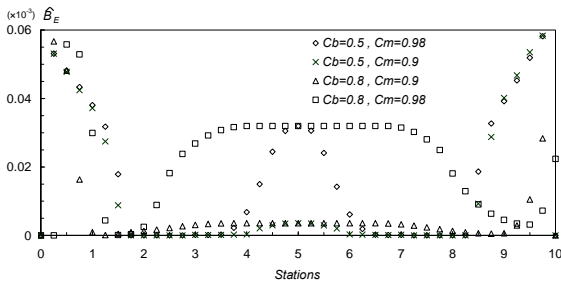


Figure 10. Effects of midship-section coefficient,  $C_m$  on eddy component of roll damping for slender ships ( $C_b=0.5$ ) and full ships ( $C_b=0.8$ ).

#### 4.3.2 Proposed Formula of the Eddy Roll Damping

By fitting these predicted eddy components a simple prediction formula is deduced as follows.

$$x_1 = B/d, x_2 = C_b, x_3 = C_m, x_4 = OG/d$$

$$\mathcal{G}_E = \frac{4 L_{pp} d^4 \mathcal{G} \varphi_a}{3 \pi \nabla B^2} C_R = \frac{4 \mathcal{G} \varphi_a}{3 \pi x_2 \cdot x_1^3} C_R$$

$$C_R = A_E \cdot \exp(B_{E1} + B_{E2} \cdot x_3^{B_{E3}})$$

$$A_E = (-0.0182x_2 + 0.0155) \cdot (x_1 - 1.8)^3 - 79.414x_2^4 + 215.695x_2^3 - 215.883x_2^2 + 93.894x_2 - 14.848$$

$$B_{E1} = (-0.2x_1 + 1.6) \cdot (3.98x_2 - 5.1525) \cdot x_4 \cdot \{(0.9717x_2^2 - 1.55x_2 + 0.723) \cdot x_4 + (0.04567x_2 + 0.9408)\}$$

$$B_{E2} = (0.25x_4 + 0.95) \cdot x_4 - 219.2x_2^3 + 443.7x_2^2 - 283.3x_2 + 59.6$$

$$B_{E3} = (46.5 - 15x_1) \cdot x_2 + 11.2x_1 - 28.6 \cdot \begin{pmatrix} 0.5 \leq C_b \leq 0.85, & 2.5 \leq B/d \leq 4.5 \\ -1.5 \leq OG/d \leq 0.2, & 0.9 \leq C_m \leq 0.99 \end{pmatrix} \quad (31)$$

#### 4.4 Bilge Keel Component ( $B_{BK}$ )

The bilge keel component is usually the largest one in the roll damping. The component creates 50-80% of the total roll damping. The component is created by shedding vortices from the sharp edges of bilge keels due to roll motion. The component can be divided into two components, the normal force component ( $B_N$ ) and the hull pressure component ( $B_S$ ). Both components are created by the same vortices from the edge of bilge keels. The former one is created by the force acting a bilge

keel, and the latter by the pressure over the hull surfaces in front and back sides of the bilge keel.

In Ikeda's method, the pressure distributions in front and back of a bilge keel are assumed on the basis of the measured ones, and are integrated over the hull surface. This means that the method may be available for any shape of cross section. Ikeda et al. experimentally found that the magnitude and distribution of the pressure created by a bilge keel significantly depends on  $Kc$ .

The roll damping due to the normal force acting on bilge keel is given by following expressions.

$$B_N = \frac{8}{3\pi} \rho r^3 l_{BK} b_{BK} \varphi_a \omega f^2 \left( 22.5 \frac{b_{BK}}{r \pi f \varphi_a} + 2.4 \right) \quad (32)$$

$$f = 1 + 0.3 \exp\{-160(1 - \sigma)\} \quad (33)$$

where  $r$  is distance from the axis of rolling to bilge keel,  $b_{BK}$  is width of bilge keel,  $l_{BK}$  is length of bilge keel and  $f$  is correction factor on bilge radius to take the velocity increase there into account.

The roll damping due to the hull pressure created by bilge keels is calculated by following equations.

$$B_S = \frac{4}{3\pi} \rho r^2 d^2 \omega \varphi_a f^2 I \quad (34)$$

$$I = \frac{1}{d^2} \int C_{PI} l_{BK} ds \quad (35)$$

where  $C_{PI}$  is pressure coefficient on hull surface. The positive pressure coefficient ( $C_{PI}^+$ ) of face of a bilge keel and the negative pressure coefficient ( $C_{PI}^-$ ) of back side of a bilge keel are given by following formulas.

$$C_{PI}^+ = 1.2 \quad (36)$$

$$C_{PI}^- = -\frac{22.5b_{BK}}{\pi f \varphi_a} - 1.2 \quad (37)$$



#### 4.4.1 Characteristics of the Bilge Keel Component

Calculated bilge keel component of the roll damping by Ikeda's method are shown in Figs. 11-13 to demonstrate the characteristics. In Figure 11 bilge keel component of the roll damping of slender ships ( $C_b=0.58$ ) and full ships ( $C_b=0.81$ ) with different midship-section coefficients are shown. In the prediction the area of bilge keels is systematically changed. The results show that the roll damping component increases with increasing area of bilge keels. For full ships the increase of the component is almost linear, but for slender ships it shows non-linearly increases. The magnitude of the component significantly depends on midship-section coefficients, but not so sensitive on block coefficient  $C_b$ .

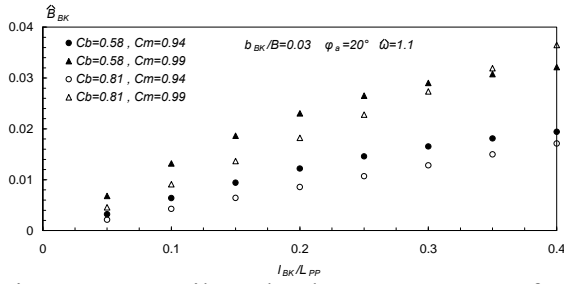


Figure 11. Bilge keel component of roll damping of slender and full ships for various bilge keel lengths and constant breadth ( $b_{BK}$ ).

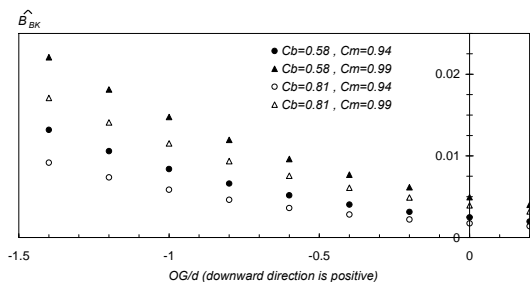


Figure 12. Effect of location of center of gravity, or roll axis on bilge keel component of roll damping.

In Figure 12, effects of location of center of gravity on bilge keel component of roll damping are shown for slender and full ships. As height of center of gravity decreases, or  $OG/d$  increases, the bilge keel component decreases. This is because relative flow speed

at bilge corner decreases and flow separation at the edge of bilge keels weakens.

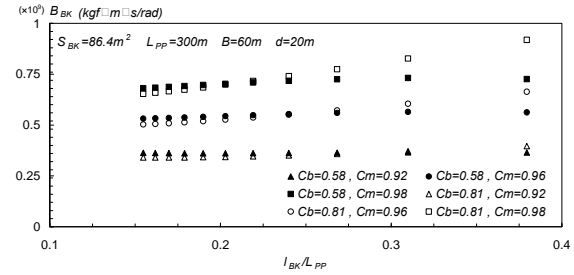


Figure 13. Bilge keel component of roll damping of slender and full ships with bilge keels of the same area ( $S_{BK}$ ) but different lengths.

In Figure 13, effects of aspect ratio (=length/breadth of a bilge keel) on the roll damping of ships with the same area bilge keels are shown. It can be seen that the component is not so sensitive with aspect ratio, but increases with increasing aspect ratio, or more slender bilge keels for full ships with large midship-section coefficients.

#### 4.4.2 Proposed Formula of the Bilge Keel Roll Damping

By fitting these predicted bilge keel components a simple prediction formula is deduced as follows.

$$x_1 = B/d, x_2 = C_b, x_3 = C_m, x_4 = OG/d, x_5 = \omega$$

$$x_6 = \phi_a \text{ (deg)}, x_7 = b_{BK}/B, x_8 = l_{BK}/L_{PP}$$

$$\hat{B}_{BK} = A_{BK} \cdot \exp(B_{BK1} + B_{BK2} \cdot x_3^{B_{BK3}}) \cdot x_5$$

$$A_{BK} = f_1(x_1, x_2) \cdot f_2(x_6) \cdot f_3(x_7, x_8)$$

$$f_1 = (-0.3651x_2 + 0.3907) \cdot (x_1 - 2.83)^2 - 2.21x_2 + 2.632$$

$$f_2 = 0.00255x_6^2 + 0.122x_6 + 0.4794$$

$$f_3 = (-0.8913x_7^2 - 0.0733x_7) \cdot x_8^2 + (5.2857x_7^2 - 0.01185x_7 + 0.00189) \cdot x_8$$

$$B_{BK1} = \{5x_7 + 0.3x_1 - 0.2x_8 + 0.00125x_6^2 - 0.0425x_6 - 1.86\} \cdot x_4$$

$$B_{BK2} = -15x_7 + 1.2x_2 - 0.1x_1 - 0.0657x_4^2 + 0.0586x_4 + 1.6164$$

$$B_{BK3} = 2.5x_4 + 15.75$$

$$\left( \begin{array}{l} 0.5 \leq C_b \leq 0.85, \quad 2.5 \leq B/d \leq 4.5 \\ -1.5 \leq OG/d \leq 0.2, \quad 0.9 \leq C_m \leq 0.99 \\ 0.01 \leq b_{BK}/B \leq 0.06, \quad 0.05 \leq l_{BK}/L_{PP} \leq 0.4 \end{array} \right) \quad (38)$$

## 5. VALIDATION OF PROPOSED METHOD

To verify the validity of the proposed method, the values of the roll damping calculated by the original Ikeda's method and the proposed method are compared on two kinds of ships. The results of these comparisons are shown in Figure 14.

These results indicate that the calculated values of roll damping by the proposed formulas are in good agreement with the roll damping calculated by the Ikeda's method, although the estimated values by using the proposed method have some errors about 10% when  $\omega$  becomes larger for the ship with  $OG/d=-0.2$  as shown in Figure 14. However, the error margin becomes small in the low-frequency range because the bilge keel component is predominant.

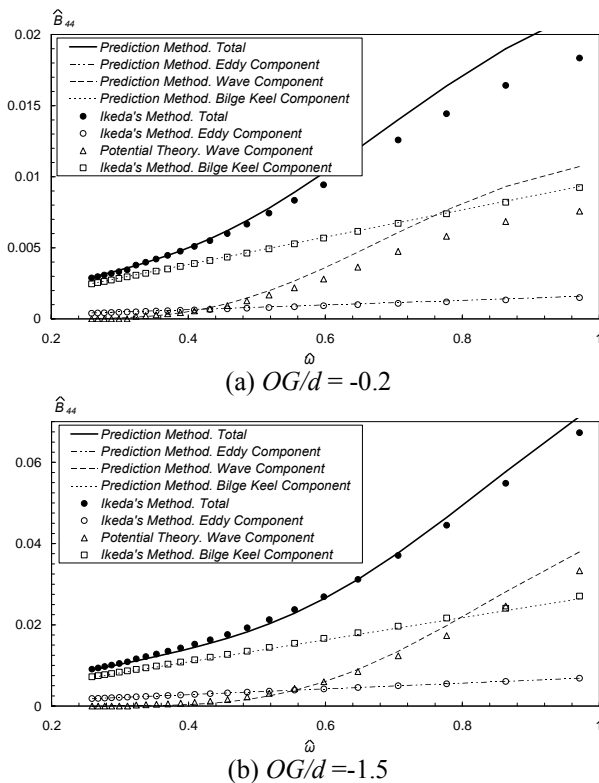


Figure 14. Comparison between Ikeda's method and proposed one of roll damping at  $L/B=6.0$ ,  $B/d=4.0$ ,  $C_b=0.65$ ,  $C_m=0.98$ ,  $\varphi_a=10^\circ$ ,  $b_{BK}/B=0.025$  and  $l_{BK}/L_{pp}=0.2$ .

The results in Figure 14 suggest that the errors come from the discrepancy of the wave component between the proposed method and the potential theory. Especially, this discrepancy grows larger on condition of  $B/d=4.5$  and  $OG/d=-0.2 \sim -0.5$ , so it should be noted for the use of the proposed method on this condition. This may be because the wave component of the roll damping intricately depends on frequency and locations of roll axis. Therefore, if more accurate prediction is needed, the calculated wave damping by any potential theory should be used.

## 6. LIMITATION OF IKEDA'S METHOD

In recent years, the number of ships that have buttock flow stern, such as large passenger ship or pure car carrier, has been increasing. In such a type of ships, however, prediction accuracy of roll damping calculated by Ikeda's method might decrease remarkably. In order to investigate its limitation, free roll decay tests are carried out by using three types of model ships, large passenger ship (LPS), modern pure car carrier (PCC) and wide breadth and shallow draft car carrier (WSPCC). The principal particulars of these ships and the body plan of large passenger ship are shown in Table 1 and Figure 15, respectively. As shown in Figure 15, the ship has shallow stern-bottom with something like a skeg.

Table 1. Principal particulars of the ships

|                  | LPS    | PCC    | WSPC   |
|------------------|--------|--------|--------|
| Scale            | 1/125  | 1/96   | 1/96   |
| $L_{OA}$ (m)     | 2.200  | 2.083  | 2.083  |
| $L_{PP}$ (m)     | 1.933  | 2.00   | 2.00   |
| Breadth (m)      | 0.287  | 0.336  | 0.378  |
| Draft (m)        | 0.067  | 0.0938 | 0.0772 |
| Displacement(kg) | 26.98  | 33.43  | 28.05  |
| GM (m)           | 0.0126 | 0.0194 | 0.063  |
| $T_{nr}$ (sec)   | 1.88   | 2.06   | 1.05   |
| $OG/d$           | -1.13  | -0.071 | -1.35  |
| $b_{BK}/Breadth$ |        | 0.0217 | 0.0217 |
| $l_{BK}/L_{PP}$  |        | 0.225  | 0.225  |

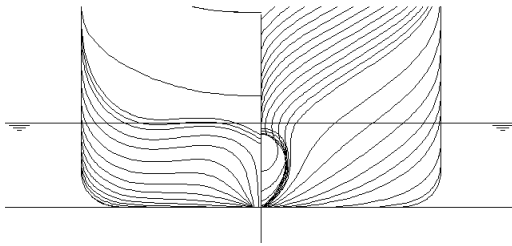
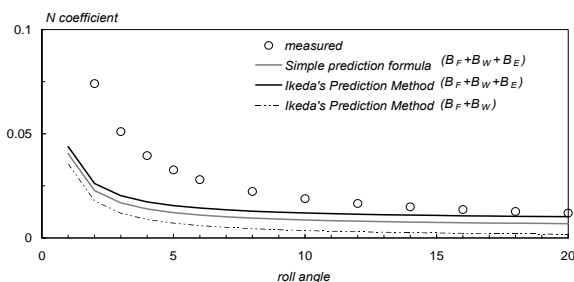
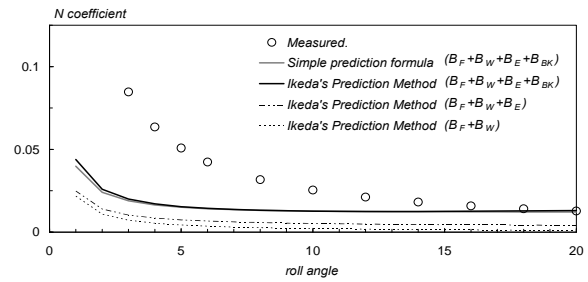


Figure 15. Body plan of large passenger ship.

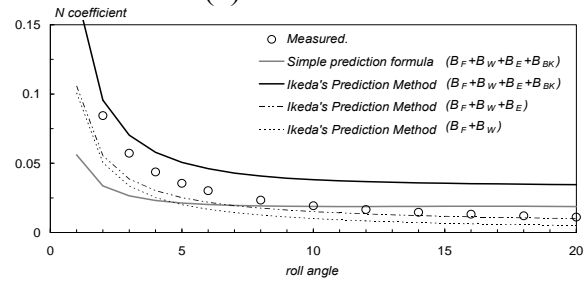
In Figure 16, the obtained results of the extinction coefficient  $N$  are shown. The results demonstrate that the accuracy of Ikeda's prediction method decrease remarkably when the roll angle is small. However, the error of roll damping becomes smaller for large passenger ship and pure car carrier in condition of large roll angle. For wide breadth and shallow draft car carrier, however, the roll damping calculated by Ikeda's prediction method is overestimated from the experimental result for whole roll angle. This is pointed out by Tanaka et al. (1981) that the effect of the bilge keel component on the roll damping significantly decreases for the wide breadth and shallow draft ships. Also, the discrepancies between the simple prediction formula and Ikeda's method are attributed to differences between methodical series model and real model ship and to using out of its possible calculating condition. Then, the extinction coefficient  $N$  of large passenger ship is relatively large even for naked hull because of relatively small bilge radius. Thus, Ikeda's prediction method is valid only in large roll angle for modern type of ships with buttock flow stern, and overestimate the roll damping for a very flat ship with large bilge keels.



(a) Large passenger ship



(b) Pure car carrier



(c) Wide breadth and shallow draft car carrier

Figure 16. Comparison of roll damping between Ikeda's method and experimental result.

## 7. CONCLUSIONS

A simple prediction method of the roll damping of ships is developed on the basis of the Ikeda's original prediction method which was developed in the same concept as a strip method for calculating ship motions in waves. Using the data of a ship,  $B/d$ ,  $C_b$ ,  $C_m$ ,  $OG/d$ ,  $\phi$ ,  $b_{BK}/B$ ,  $l_{BK}/L_{PP}$ ,  $\phi_a$ , the roll damping of a ship can be approximately predicted. Moreover, the limit of application of Ikeda's prediction method to modern ships that have buttock flow stern is demonstrated by the model experiment. The computer program of the method can be downloaded from the Home Page of Ikeda's Labo.

([http://www.marine.osakafu-u.ac.jp/~lab15/roll\\_damping.html](http://www.marine.osakafu-u.ac.jp/~lab15/roll_damping.html)).

## 8. ACKNOWLEDMENTS

This work was supported by a Grant-in Aid for Scientific Research of the Japan Society for Promotion of Science (No. 18360415).



The authors wish to express sincere appreciation to Prof. N. Umeda of Osaka University for valuable suggestions to this study.

## 9. REFERENCES

- Himeno, Y (1981), "Prediction of Ship Roll Damping – State of the Art-, Report of Dept. of Naval Architecture & Marine engineering, the University of Michigan, No.239
- Ikeda, Y., Himeno, Y., Tanaka, N (1976). "On Roll Damping Force of Ship -Effects of Friction of Hull and Normal Force of Bilge Keels-", Journal of the Kansai Society of Naval Architects, Japan No.161, pp 41-49.
- Ikeda, Y., Komatsu, K., Himeno, Y., Tanaka, N (1977a). "On Roll Damping Force of Ship - Effects of Hull Surface Pressure Created by Bilge Keels-", Journal of the Kansai Society of Naval Architects, Japan No.165, pp 31-40
- Ikeda, Y., Himeno, Y., Tanaka, N (1977b). "On Eddy Making Component of Roll Damping Force on Naked Hull", Journal of The Society of Naval Architects, Japan No.142, pp 59-69
- Ikeda, Y., Himeno, Y., Tanaka, N (1978). "Components of Roll Damping of Ship at Forward Speed", Journal of The Society of Naval Architects, Japan No.143, pp 121-133
- Ikeda, Y., Fujiwara, T., Himeno, Y., Tanaka, N., "Velocity Field around Ship Hull in Roll Motion", Journal of the Kansai Society of Naval Architects, Japan No.171, pp 33-45
- Ikeda, Y (1982), "Prediction Method of Roll Damping", Report of Dept. of Naval Architecture, University of Osaka Prefecture
- Ikeda, Y. (1984). "Roll damping", 1ST Symposium of Marine Dynamics Research Group, Japan, pp 241-250
- Kawahara, Y., (2008). "Characteristics of Roll Damping of Various Ship Types and A Simple Prediction Formula of Roll Damping on the Basis of Ikeda's Method", The 4<sup>th</sup> Asia-Pacific Workshop on Marine Hydrodynamics, Taipei, pp 79-86